Food Chemistry 400 (2023) 134073

Contents lists available at ScienceDirect

Food Chemistry

journal homepage: www.elsevier.com/locate/foodchem

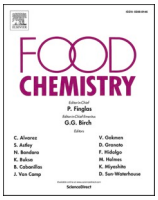

Antioxidant starch composite films containing rice straw extract and cellulose fibres

Pedro A.V. Freitas *, Consuelo González-Martínez, Amparo Chiralt

Institute of Food Engineering for Development, Universitat Politècnica de València, 46022 Valencia, Spain

ARTICLE INFO

Keywords:
Bioactive constituents
Active extracts
Thermoplastic starch films
Valorisation of residues
Green extraction methods
Circular economy

ABSTRACT

Antioxidant aqueous rice straw (RS) extract was obtained by a combined ultrasound-reflux heating process and cellulose fibres (CF) were purified by bleaching the extraction residue. Both fractions were incorporated into corn starch to obtain films by melt blending and compression moulding. CF (at 3 % wt.) greatly increased the elastic modulus (by 200 %) and tensile strength at break (by 100 %) while reducing film stretchability. Films with CF exhibited the greatest barrier capacity to water vapour and oxygen. The incorporation of RS extract (at 4, 6 and 8 % wt.) plasticised the film's amorphous phase, but also reinforced the matrix to a certain extent. The active films showed a high degree of UV absorption and DPPH radical scavenging capacity. Mono-dose sunflower oil bags were obtained with films with CF and RS extracts that, to a great extent, prevent oil oxidation in an accelerated oxidative test under UV radiation throughout 50 days.

1. Introduction

The valorisation of agricultural waste is of growing interest in the context of the circular economy. One potential use of the fractions obtained from lignocellulosic residues is that of the development of packaging materials with circulating resources (Mochane et al., 2021), thus helping to limit the disposal of waste in landfills and to eliminate greenhouse gas emissions while valorising the vegetal residues (Mak et al., 2020). One potential application of these residues is based on both their cellulosic content and bioactive phytochemicals, which could be used for producing packaging materials with improved functions, such as reinforced mechanical properties and antioxidant or antimicrobial activity. Of the agricultural waste, rice straw (RS) is the third-largest residue from agriculture after sugarcane bagasse and maize straw, presenting problematic waste management and non-economic value. Due to its high cellulose content (37 %, Freitas et al. (2022a)), RS is a good source of cellulosic components (microfibres, nanocrystals), which could be used as reinforcing materials for enhancing the films mechanical and barrier properties (Freitas et al. 2021; Freitas et al., 2022a). The lignocellulosic fraction consists of a complex matrix made up of crystalline cellulose microfibrils as the primary fibre component linked to a cementing matrix composed of hemicellulose and lignin (Chen et al., 2011), which have to be removed to obtain the purified cellulose. Several authors (Perumal et al., 2018; Freitas et al., 2022a) incorporated nanocrystals or cellulose fibres (CF) from RS into different polymer matrices, such as polyvinyl alcohol/chitosan, or starch/methylcellulose/gum Arabic blended films, to analyse their reinforcing capacity. Their incorporation into the polymeric matrix led to films which are stronger and have greater elastic modulus due to the fibre entanglement, which plays an important role in the force transferring from the matrix to fibrils and from fibrils to fibrils (Balakrishnan et al., 2018). Moreover, the RS has been shown to be a valuable source of phenolic compounds, such as ferulic, *p*-coumaric, protocatechuic or caffeic acids, tricin, pyrogallol or vanillin, among others (Menzel et al., 2020). Most of these phenolic compounds exhibited antioxidant and/or antimicrobial activity and can be obtained from RS by water extraction, leading to aqueous extracts with proven antioxidant capacity (Menzel et al., 2020; Freitas et al., 2020). These active extracts could be incorporated into biodegradable polymers for the purposes of obtaining sustainable active packaging materials for food packaging applications. These active packages could contribute to enhancing food preservation by adding new functionalities to the materials, such as antioxidant and antimicrobial activities, which could extend the shelf-life and enhance the safety of the foodstuff.

Starch is a biodegradable polymer, thermoplastic in nature, and considered a valuable material for food packaging. The major disadvantages of the starch-based films are related to their low mechanical resistance, water sensitivity and solubility and limited water vapour

* Corresponding author.
E-mail address: pedvidef@doctor.upv.es (P.A.V. Freitas).

https://doi.org/10.1016/j.foodchem.2022.134073
Received 27 June 2022; Received in revised form 23 July 2022; Accepted 28 August 2022
Available online 5 September 2022

barrier properties. Nevertheless, these films exhibit a great oxygen barrier capacity, which is essential for the prevention of oxidative processes in foodstuffs. This can be enhanced by incorporating both natural antioxidant compounds, which can act as oxygen or radical scavenging agents, and cellulose fibres (CF) (Talón et al., 2019). Therefore, it is possible to address a new strategy to develop sustainable packaging materials by using biodegradable polymers, such as starch, and lignocellulosic waste fractions, such as cellulose components and bioactive extracts. This is aligned with the circular bioeconomy, reusing agricultural waste, and the Sustainable Development Goals as defined by the United Nations (Economic & Affairs, 2018). The use of these RS fractions in starch-based films could extend the shelf-life of perishable products that are highly susceptible to lipid oxidation, such as unsaturated sunflower oils (with 70 % unsaturated fatty acids), while enhancing the barrier and mechanical properties of the packaging material. This strategy is also in line with the current consumer demand for non-synthetic additives and contributes to proper environmentally-friendly waste management, producing added-value materials, reducing food losses, and boosting the circular bioeconomy (Ng et al., 2015).

Very few studies incorporating both cellulose and bioactive fractions from agricultural waste have been carried out to the best of our knowledge. Menzel (2020) studied the improvement of starch film properties by using a three-principle approach: antioxidants, cross-linking, and reinforcement, and obtained films with valuable phenolic compounds and cellulose fibres from sunflower hulls, and citric acid as the crosslinker. Films had inherent antioxidant activity and a better mechanical performance, in terms of stress resistance and extensibility, while an increase in the branch-chain length of citric acid cross-linked starch was observed. Sá et al. (2020) developed films based on bacterial cellulose produced from cashew apple juice and lignin and cellulose nanocrystals from the cashew tree pruning fibre. Lignin and cellulose nanocrystals enhanced the tensile and barrier properties of the films, while lignin provided films with UV-absorbing and antioxidant properties.

Therefore, the aims of this study were to use valorised fractions of RS (antioxidant aqueous extract and CF) to improve the functional properties of starch-based films and to evaluate how well they prevent sunflower oil oxidation. To this end, films were obtained by melt blending and compression moulding and characterised as to their microstructure, mechanical, optical, and barrier properties, as well as their thermal behaviour and antioxidant activity. Finally, the performance of the films in the prevention of sunflower oil oxidation was evaluated in mono-dose oil bags submitted to an accelerated oxidation test.

2. Material and methods

2.1. Chemicals

Corn starch (27 % amylose) was supplied by Roquette (Roquette Laisa, Spain). Glycerol, acetic acid, sodium carbonate (Na_2CO_3) (99.5 % purity), di-phosphorus pentoxide (P_2O_5), and magnesium nitrate ($Mg(NO_3)_2$) were supplied by PanReac Quimica S.L.U. (Castellar del Vallés, Spain). Gallic acid, Folin-Ciocalteau reagent (2 N), methanol (>99.9 purity), 2,2-Diphenyl-1-picrylhydrazyl (DPPH), sodium chlorite, 2-thiobarbituric acid (>98 % purity), and 1,1,3,3-tetramethoxypropane were purchased from Sigma-Aldrich (St. Louis, MO, USA). Iodine (99.5 % purity) was obtained by Acros Organics® (Geel, Belgium).

2.2. Obtaining rice straw fractions

Aqueous extract and cellulose fibres were obtained from rice straw (RS), as described in previous studies (Freitas et al., 2020; Freitas et al., 2022a). RS (*Oryza sativa* L.), J. *Sendra* var., was obtained from L'Albufera rice fields (Valencia, Spain) and was vacuum dried (0.8 mmbar, 50 ± 2 °C, 16 h), ground using a grinding machine (IKA, model M20, IKA Werke GmbH & Co. KG, Staufen, Germany), and sieved (particles of under 0.5 mm) before the extraction process.

2.3. Aqueous extract

Aqueous RS extract was obtained according to Freitas et al. (2020), by applying a sequential combination of ultrasound followed by a reflux heating step, using a RS: distilled water ratio of 1:20 (w/v). The aqueous dispersion was sonicated at 25 °C (using an ice bath) for 30 min using a probe high-intensity ultrasonic homogeniser (Vibra CellTM VCX750, 750 W power, Sonics & Material, Inc., Newtown, CT, USA), operating at a frequency of 20 kHz, 40 % sonication amplitude. Afterwards, the plant suspension was heated at 100 °C for 1 h using a typical reflux heating device. The suspension was filtered with a qualitative filter (Filterlab), and the filtrate was freeze-dried (Telstar, model LyoQuest-55) at −65 °C and 0.8 mbar for 72 h. The freeze-dried RS extract was stored in a dark bottle at 4 ± 2 °C until further use. The total phenolic content (TPC) of the RS extract was 37.1 ± 0.4 mg gallic acid equivalent (GAE) per g of freeze-dried extract, according to the Folin-Ciocalteu method (Freitas et al. 2020). The antioxidant capacity of the extract, evaluated by the 2,2-Diphenyl-1-pikryl-hydrazyl (DPPH) radical scavenging method (Brand-Williams et al., 1995; Menzel et al., 2019), and expressed as EC_{50} value, was 6.3 ± 0.3 mg freeze-dried extract/mg DPPH. The EC_{50} value is defined as the ratio of sample to DPPH required to reduce the DPPH concentration by 50 % when reaction stability is achieved.

2.4. Cellulose fibres

The insoluble residue from the aqueous extraction of RS (section 2.2.1) was dried (40 °C for 48 h), and used to obtain cellulose fibres (CF), as reported by Freitas et al. (2022a). Briefly, the bleaching step was performed by mixing the lignocellulosic residue and the bleaching solution at 5 % (w/v), which consisted of a solution of equal parts of sodium chlorite solution (1.7 %, w/v), acetate buffer solution (2 N), and distilled water. The mixture was heated at reflux for 4 cycles of 4 h each. After the bleaching cycles, the bleached cellulose fraction was dried at 35 °C for 48 h and ground using a milling machine (pulses of 2 s for 20 min, model M20, IKA Werke GmbH & Co. KG, Staufen, Germany) to obtain the CF. The chemical composition of the CF, analysed according to the NREL/TP-510–42,618 method (Sluiter, 2008), was 66 % cellulose, 10 % hemicellulose, 5 % lignin, and 5 % ashes (Freitas et al. 2022a). Likewise, the morpho-geometric characteristics of CF evaluated by FESEM showed major cumulative frequencies of lengths and thicknesses below 200 μm and 5–15 μm, respectively (Freitas et al., 2021).

2.5. Film preparation

Thermoplastic starch-based films were obtained with and without CF at 3 % (wt.) with respect to the total starch mass, since this was the CF ratio that gave rise to the maximum reinforcing capacity in a previous study (Freitas et al., 2021). Likewise, RS extract at 0, 4, 6, and 8 % wt. (with respect to the total starch mass) was incorporated into TPS films with and without CF. Films were obtained by melt blending of the components and subsequent compression moulding, using glycerol as plasticiser at 30 % wt. with respect to the total starch mass. Preconditioned starch (P_2O_5 at 25 °C for 7 days) was firstly mixed with the other film components and melt-blended in an internal mixer (HAAKETM PolyLabTM QC, Thermo Fisher Scientific, Karlsruhe, Germany) at 130 °C and 50 rpm for 10 min. For each treatment, the obtained solid mixture was milled and conditioned at 25 °C and 53 % relative humidity (RH) (using $Mg(NO_3)_2$ saturated solution) for one week. Thereafter, the milled pellets (4 g) were put onto Teflon sheets and compression-moulded in a heat plates hydraulic press (Model LP20, Labtech Engineering, Thailand) as follows: preheating at 160 °C for 3 min, compression at 30 bars and 160 °C for 2 min, followed by 130 bars for 6 min (160 °C), and then a final cooling to 80 °C. All films were conditioned at 25 °C and 53 % RH for one week before their

characterisation.

2.6. Film characterisation

2.6.1. Film microstructure

A Field Emission Scanning Electron Microscope (ULTRATM 55, Zeiis, Oxford Instruments, UK) was used to observe the morphologies of the cross-sections of the films. The conditioned samples (P_2O_5 for 1 week at 25 °C) were cryo-fractured by immersion in liquid nitrogen and then covered with platinum using an EM MED020 sputter coater (Leica Bio-Systems, Barcelona, Spain). The micrographs were taken under vacuum and at 2.0 kV acceleration voltage.

2.6.2. Thermal analysis

A TGA analyser (TGA 1 Stare System analyser, Mettler-Toledo, Switzerland) was used to perform the thermogravimetric analysis (TGA) of the films. Conditioned film samples (P_2O_5 for 1 week at 25 °C) of about 3–5 mg were weighed in alumina pans and heated from 25 to 700 °C at a heating rate of 10 °C.min^{-1} under a nitrogen atmosphere (10 mL.min^{-1}). The thermal stability for each treatment was evaluated in terms of the initial (T_{on}) and maximum degradation rate (T_p) temperatures, and the residual mass by analysing the TGA curves and their first derivative (DTGA). The measurements were taken in duplicate.

The phase transitions of the films were analysed by differential scanning calorimetry (DSC) using a DSC Stare System analyser (Mettler-Toledo GmbH, Switzerland). Dry conditioned samples (5–7 mg) were sealed in aluminium pans and heated from 25 to 160 °C, then cooled to 25 °C, and subsequently heated again to 160 °C at a heating rate of 10 °C.min^{-1} under nitrogen atmosphere (10 mL.min^{-1}). The analyses were performed in duplicate.

2.6.3. Equilibrium water content and water solubility

The equilibrium water content of the films, conditioned at 53 % RH and 25 °C for two weeks, was determined as described by Freitas et al. (2021). Film samples (3 cm × 3 cm) were dried at 60 °C for 24 h, and then placed into desiccators containing P_2O_5 at 25 °C for two weeks. For each treatment, the moisture content was determined from the total mass loss of the film after the drying process. The measurements were taken in triplicate.

The water solubility of the films was determined according to the methodology described by Talón et al. (2017). Conditioned film samples (P_2O_5 at 25 °C for two weeks) of about 2 cm × 2 cm were placed on a mesh and immersed in a crucible containing 30 mL of distilled water at 25 °C for 24 h. Thereafter, the crucibles were dried in an oven (J. P. Selecta, S. A., Spain) at 60 °C for 48 h and then placed in desiccators containing P_2O_5 at 25 °C for one week. The water solubility of the films was expressed as the mass of solubilised film per 100 g of dry film. The measurements were taken in triplicate.

2.6.4. Tensile properties

The tensile properties of the films, typically tensile strength at break (TS), elongation at break (E), and elastic modulus (EM), were determined according to ASTM D882 (ASTM, 2012) using a universal test machine (TA.XTplus model, Stable Micro Systems, Haslemere, England). Before the analysis, the films were conditioned at 25 °C and 53 % RH for two weeks. The film samples (25 mm × 100 mm) were grabbed by two grips initially separated by 50 mm and stretched at a crosshead speed of 50 mm.min^{-1}. Eight samples were evaluated for each formulation.

2.6.5. Barrier properties

The oxygen permeability (OP) of the films was determined according to ASTM D3985-05 (ASTM, 2010) methodology using an Oxygen Permeation Analyser (Model 8101e, Systech Illinois, Illinois, USA) at 25 °C and 53 % RH. The area of the films was 50 cm^2 and the oxygen transmission rate (OTR) was obtained every 15 min until equilibrium was reached. The measurements were taken in duplicate.

The water vapour permeability (WVP) of the films, expressed as g.mm.kPa^{-1}h^{-1}.m^{-2}, was obtained gravimetrically according to ASTM E96/E96M (ASTM, 2005), with modifications described by McHugh et al. (1993). Conditioned film samples (at 53 % RH and 25 °C, for two weeks) were cut (Ø = 3.5 cm), sealed in Payne permeability cups (Elcometer SPRL, Hermelle/s Argenteau, Belgium) containing 5 mL of distilled water (100 % RH), and placed into desiccators at 25 °C and 53 % RH ($Mg(NO_3)_2$). The cups were weighed periodically (ME36S, Sartorius, ± 0.00001 g, Fisher Scientific, Hampton, NH, USA) every 1.5 h for 27 h. The WVP of the films were determined from the water vapour transmission rate, which was determined from the slope of the weight loss *vs* time curve. For each treatment, the analysis was performed in triplicate.

2.6.6. Optical properties

The optical properties of the films were obtained based on the Kubelka-Munk theory of multiple scattering using a spectrocolorimeter (CM-3600d, Minolta Co., Japan). The reflection spectra (R) of the films from 400 to 700 nm were obtained on white (R_g) and black (R_0) backgrounds. The internal transmittance (T_i) and the infinite reflectance (R_∞) were obtained according to Eqs. 1–4. The film colour coordinates L^* (lightness), a^* (redness-greenness), and b^* (yellowness-blueness) were obtained from the R_∞ spectra, considering observer 10° and illuminant D65. Finally, the psychometric colour coordinates were obtained: chroma (C_{ab}^*) (Eq. (5)), hue angle (h_{ab}^*) (Eq. (6)), and total colour difference (ΔE^*) (Eq. (7)).

The light barrier properties of the films were evaluated by measuring the UV–vis spectra ranging from 200 to 900 nm using a UV–visible spectrophotometer (Evolution 201, Thermo Scientific) operating in light transmission mode.

$$T_i = \sqrt{(a - R_0)^2 - b^2} \tag{1}$$

$$R_\infty = a - b \tag{2}$$

$$a = \frac{1}{2}\left[R + \left(\frac{R_0 - R + R_g}{R_0 \times R_g}\right)\right] \tag{3}$$

$$b = \sqrt{a^2 - 1} \tag{4}$$

$$C^* = \sqrt{a^{*2} + b^{*2}} \tag{5}$$

$$h^* = arctg\left(\frac{b^*}{a^*}\right) \tag{6}$$

$$\Delta E^* = \sqrt{(\Delta L^*)^2 + (\Delta a^*)^2 + (\Delta b^*)^2} \tag{7}$$

Where $\Delta L^* = (L^* - L_0^*)$; $\Delta a^* = (a^* - a_0^*)$; $\Delta b^* = (b^* - b_0^*)$; and L_0^*, a_0^*, and b_0^* are the colour coordinates of the fillets at initial time.

2.6.7. Phenolic content and antioxidant properties of the films

The total content of phenolic compounds in the processed films was determined by dissolving a determined mass of films in distilled water and quantifying the total phenolic compounds released into the aqueous media and their corresponding antioxidant capacity as described by (Collazo-Bigliardi et al., 2019), with some modifications. Conditioned film samples (P_2O_5 at 25 °C for two weeks) of about 1.5 g were immersed in 100 mL of distilled water and stirred in dark bottles for 16 h at 20 ± 2 °C. Afterwards, the samples were filtered (Filter-Lab, 0.45 μm) and the filtrate analysed as to the TPC and the radical scavenging activity (EC_{50}), as described in section 2.2.1. All measurements were taken in triplicate.

2.6.8. Prevention of sunflower oil oxidation with mono-dose film bags

The antioxidant properties of the films with RS extracts were validated by packaging sunflower oil in thermo-sealed mono-dose bags of

the films and storing it for 50 days under accelerated oxidation conditions. To this end, TPS-8 and TPScf-8 films, and their corresponding black samples without RS extract, TPS and TPScf, were selected, based on their antioxidant content and oxygen barrier capacity. Film samples, 7 cm × 11 cm in size, were previously thermo-sealed using a vacuum sealer (Vacio Press, Saeco) to obtain rectangular bags. Then, 7 mL of commercial sunflower oil was placed into the bags and thermo-sealed (Fig. 3). To validate the oxidation conditions, open Petri dishes containing 7 mL of sunflower oil was used as sample control. The bags were stored in a chamber at 30 °C, 53 % RH, and exposed to fluorescent light (intensity of 1000–1500 lx) at 30 cm from the samples for 50 days. The oxidative stability of the packaged oil samples was evaluated in terms of the peroxide index and the 2-thiobarbituric acid reactive substance (TBARS) index on days 0, 10, 20, 35, and 50 of storage. The oil samples from two bags of each film were analysed at each storage time.

2.6.8.1. Peroxide index. The peroxide index of the sunflower oil was determined according to the titrimetric method (IUPAC - International Union of Pure & Applied Chemistry). For this purpose, oil samples of about 1 g were dissolved with 10 mL organic solvent consisting of glacial acetic acid: decan-1-ol in a ratio of 3:2 (v/v). 200 µL of saturated potassium iodide solution was added and kept in the dark for 1 min. Afterwards, 50 mL distilled water was added, and the dispersion was titrated using an automatic titrator (Titrando, Metrohm Ion Analysis,

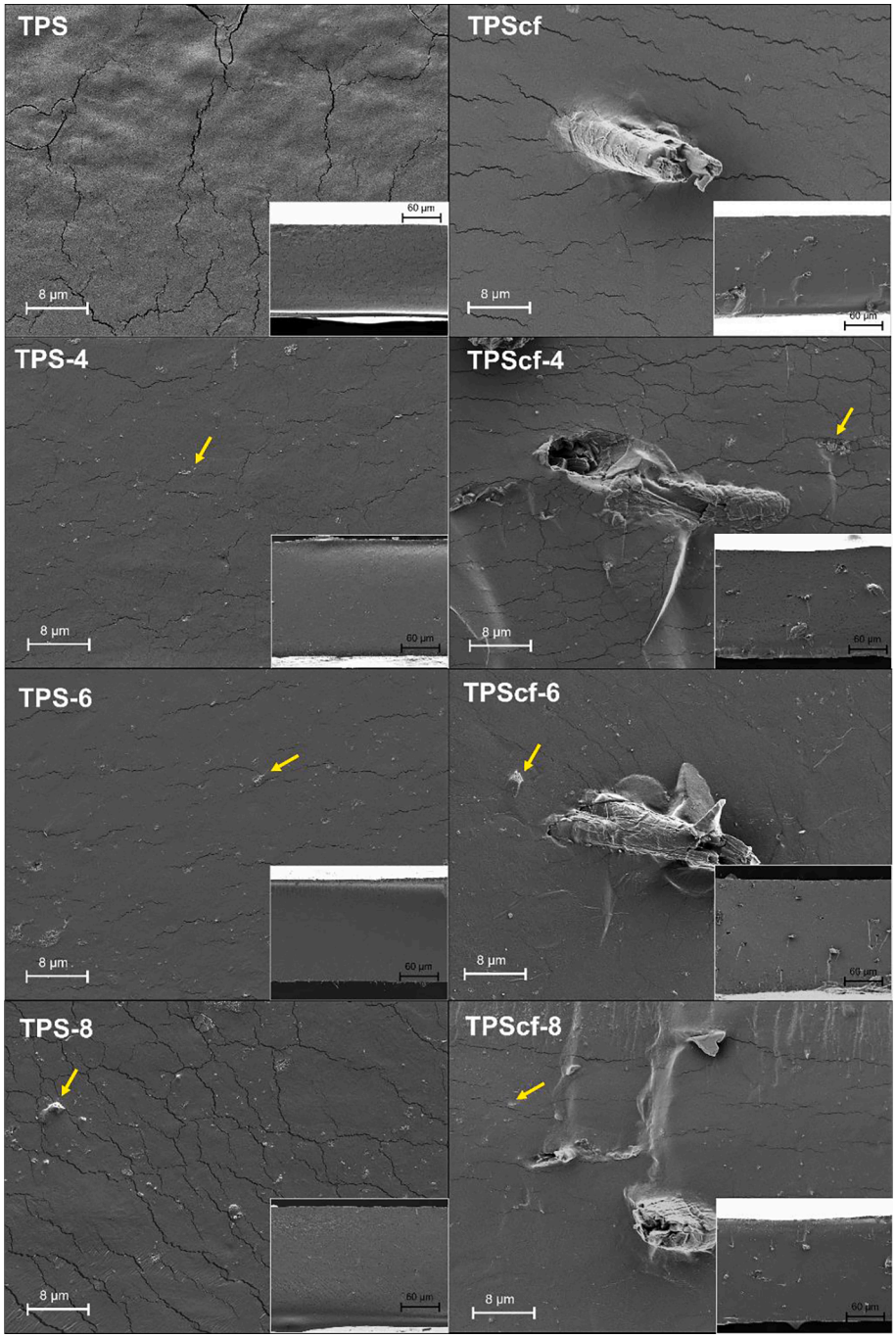

Fig. 1. FESEM micrographs (2000x magnification) of films with different RS extract ratios (0, 4, 6 and 8 % w/w) with (right) and without (left) cellulose fibres (CF). Arrows marked the RS extract aggregates formed in the starch matrix. Embedded micrographs (400x magnification) show a complete image of the film's cross section.

Switzerland) with 0.01 or 0.001 M sodium thiosulfate, depending on the expected peroxide concentration. The procedure was performed in duplicate for each treatment.

2.6.8.2. The 2-thiobarbituric acid reactive substance (TBARS) assay. The TBARS index of the oil samples was performed according to the method previously described by Papastergiadis et al. (2012). Briefly, 1 g of sample was mixed with 5 mL distilled water, vortexed for 2 min, and centrifuged at 5000*g* for 5 min. Subsequently, the aqueous phase was separated and collected, and the procedure was repeated twice. 2 mL of the aqueous extract was mixed with 2 mL of 2-thiobarbituric acid solution (46 mM) in a test tube and heated at 100 °C for 35 min. Afterward,

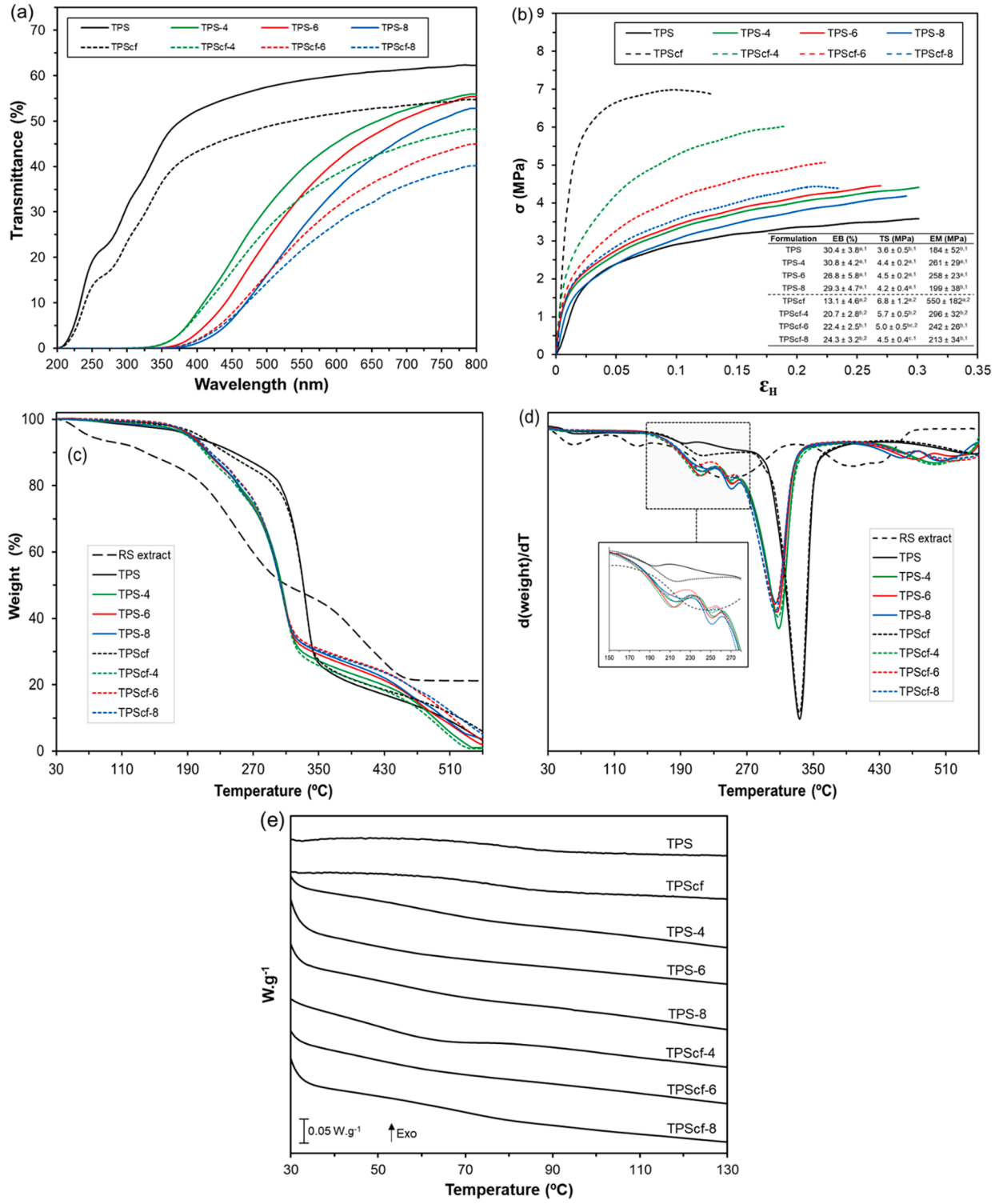

Fig. 2. (a) UV–vis spectra, (b) Stress–strain curves and tensile properties (inserted table) (EB, TS, and EM), (c) TGA curves, (d) DTGA first derivative curves, and (e) second heating DSC thermograms of thermoplastic starch films with different contents of RS extract (0, 4, 6, and 8 % wt.) with (continuous lines) and without (dashed lines) CF. For the mechanical properties, different subscript letters indicate significant differences between samples of the same group (TPS or TPScf films). Different numbers indicate significant differences between TPS and TPScf samples with the same ratio of RS extract (Tukey test, $p < 0.05$).

the tubes were cooled to room temperature and the absorbance was obtained at 532 nm. The TBARS index was expressed as mg malonaldehyde (MDA) per kg of sunflower oil, using 1,1,3,3-tetramethoxypropane as standard (0.5 – 12 μM).

2.7. Statistical analysis

The experimental data were analysed through a multifactorial analysis of variance at a 95 % confidence level using the Minitab Statistical Program (version 17). Tukey's studentised range (HSD) test, considering the least significant difference (α) of 5 %, was applied to determine whether there were significant differences among the samples.

3. Results and discussion

3.1. Film microstructure and appearance

The microstructure of the obtained films can be observed in Fig. 1, where the FESEM micrographs of the different samples are shown. The typical homogeneous matrix of the starch film was obtained when no cellulosic fibre or extract was incorporated into the formulation, as reported by other authors (Tavares et al., 2019). The incorporation of the RS extract in different ratios provoked slightly more heterogeneous films, in which small particle aggregates appeared dispersed in the starch matrix (arrows in Fig. 1). The number of particles increased as the extract ratio rose in the films, which suggests that the RS extract compounds were only partially compatible with the starch matrix and separated from the starch continuous phase during the melt blending process. Some compounds were homogeneously incorporated, but some separated as visible aggregates in the FESEM micrographs. Similar behaviour was observed in PLA films which incorporated RS extract (Freitas et al. 2022b). The incorporation of 3 % CF into the films also produced a heterogenous structure (Fig. 1), showing the large fibres embedded in the starch matrix. A good interfacial adhesion can be observed between CF particles and the polymer matrix, as deduced from the micrographs in which no CF separation can be seen to have occurred during the film cryofracture, both in films with and without RS extract.

Incorporating both RS fractions provoked notable changes in the film-light interactions that were reflected in the differences of the internal transmittance and colour between the films. Fig. 2a shows the film transmittance in the UV–vis wavelength range, where these differences can be appreciated for the films with CF and RS extracts with respect to the TPS film. As expected, CF led to a decrease in the transmittance of the TPS films, in the complete wavelength range, whereas the RS extract absorbed UV radiation ($\lambda < 400$ nm) and low wavelength VIS radiation intensely, giving rise to the appearance of colour. Films containing both CF and RS extracts had the lowest transmittance values, which represents a good light barrier able to protect foods sensitive to light induced oxidative processes. Both light dispersions provoked by the dispersed particles and selective absorption due to the coloured compounds of the RS extract contributed not only to the film's appearance but also to their light barrier capacity.

The colour parameters (Lightness: L^*, Chrome: C_{ab}^* and hue: h_{ab}^*) of the films are shown in Table 1, in which the impact of light interactions with the films on their appearance may be quantified through the total colour difference with respect to the TPS films without RS components. The greatest colour difference was observed for films with 8 % RS extract with and without CF; this, however, decreased when the ratio of RS extract was reduced, in line with the lower content of coloured compounds from the RS extract. The incorporation of CF did not provoke relevant colour differences in the films, only promoting a slightly more vivid colour (higher C_{ab}^* values) due to the enhancement of light scattering by the dispersed fibres. Nevertheless, this effect was completely attenuated in films containing RS extract, where the presence of CF did not imply significant colour changes with respect to the corresponding film without fibres, despite the small differences observed in the transmittance spectra. In contrast, the RS extract led to a reduction in the film's lightness, an increase in colour saturation (C_{ab}^*) and a displacement of the hue value (h_{ab}^*) towards a redder colour, proportionally to the extract ratio in the films.

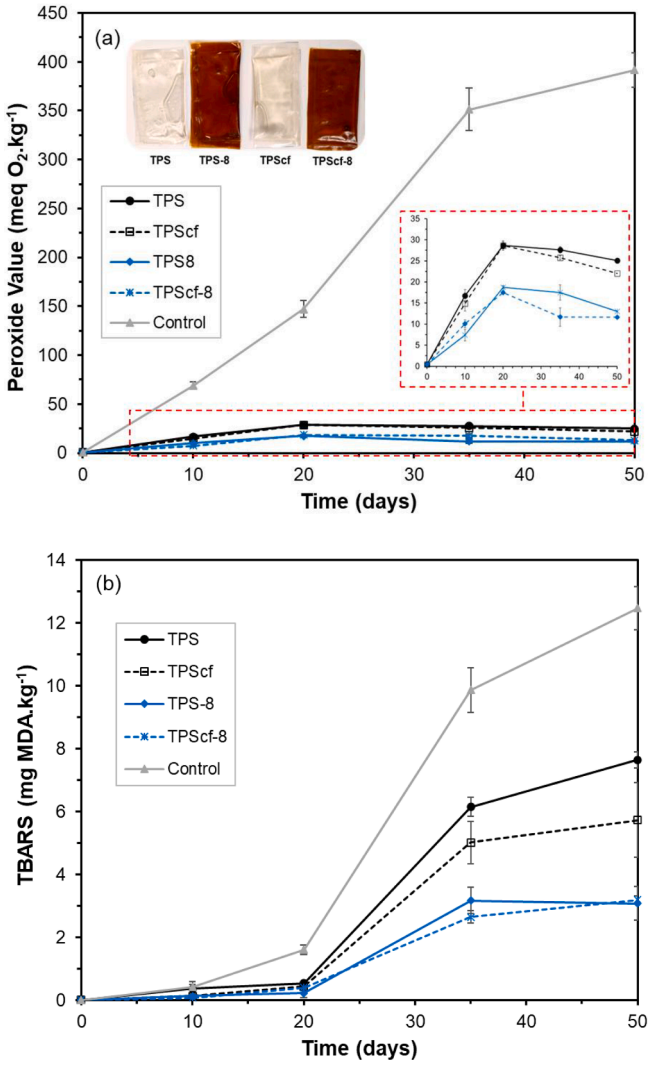

Fig. 3. Peroxide index and TBARs values of sunflower oil packaged in starch films containing or not RS extract (at 8 % wt.) and CF, compared to the open control samples, throughout 50 days of storage.

Table 1
Colour parameters (Lightness: L^*, Chrome: C_{ab}^* and hue: h_{ab}^*) and total global difference (ΔE^*) of TPS films with different RS extract ratios (0, 4, 6, and 8 % wt.) with and without CF.

Formulation	L^*	C_{ab}^*	h_{ab}^*	ΔE^*
TPS	$88.5 \pm 0.1^{a,1}$	$7.57 \pm 0.10^{a,2}$	$92.5 \pm 0.1^{a,1}$	–
TPS-4	$68.9 \pm 1.4^{b,1}$	$43.2 \pm 1.4^{c,1}$	$80.6 \pm 0.1^{b,1}$	40.4 ± 2.0^{d}
TPS-6	$60.4 \pm 0.7^{c,1}$	$48.7 \pm 0.5^{d,1}$	$74.3 \pm 1.2^{c,1}$	50.1 ± 0.7^{bc}
TPS-8	$55.5 \pm 2.0^{d,1}$	$47.7 \pm 0.9^{d,1}$	$70.0 \pm 1.8^{d,1}$	52.5 ± 0.6^{a}
TPScf	$88.1 \pm 0.2^{a,1}$	$8.3 \pm 0.5^{b,1}$	$92.6 \pm 0.3^{a,1}$	0.8 ± 0.4^{e}
TPScf-4	$67.9 \pm 1.2^{b,1}$	$42.8 \pm 0.8^{d,1}$	$80.1 \pm 0.8^{b,1}$	40.8 ± 1.2^{d}
TPScf-6	$60.5 \pm 0.8^{c,1}$	$47.7 \pm 0.2^{d,1}$	$74.3 \pm 0.7^{c,1}$	49.2 ± 0.6^{c}
TPScf-8	$59.3 \pm 0.7^{c,1}$	$49.4 \pm 0.6^{d,1}$	$72.9 \pm 0.8^{c,1}$	51.4 ± 0.3^{ab}

Different subscript letters indicate significant differences between samples of the same group (TPS or TPScf films). Different numbers indicate significant differences between TPS and TPScf samples with the same ratio of RS extract (Tukey test, $p < 0.05$).

3.2. Thermal behaviour of the films

The DSC thermograms (second heating step) of different samples showed the glass transition of starch (Fig. 2e). The T_g midpoint values are shown in Table S1, where the plasticising effect of the RS extract on the TPS matrix may be observed, whereas no significant changes in the T_g were provoked by the addition of CF. The observed T_g values of TPS are in the range reported by other authors (Collazo-Bigliardi et al. 2019; Ordoñez et al., 2021), whereas the incorporation of the RS extract (at 4–8 %) reduced T_g by about 15 °C. This suggests that the extract compounds provoked a reduction in the mean molecular weight of the starch matrix, increasing the free-volume of the polymer chains and promoting their molecular mobility (Dalnoki-Veress et al., 2001). Other studies (Menzel et al., 2020) also reported the plasticising effect of the RS aqueous extract on thermoprocessed potato starch films. In this study, lower molar mass and shorter amylose branches were determined in the glycerol plasticised starch films, which explained the reduction in the glass transition of the starch matrix. The presence of phenolic acids in the extract promoted the degradation of starch during the melt-blending process, whereas glycerol was observed to exert a protective effect, in agreement with what has been reported by other authors (Carvalho et al., 2003).

Fig. 2c shows the TGA curves of both the different films and of the RS extract. The TGA curves of all the films exhibited the typical degradation behaviour of glycerol-plasticised starch with a first mass loss step, before the main degradation peak, corresponding to the loss of bonded water and glycerol (2 % wt.). The thermal stability of the starch matrix was also affected by the presence of the RS extract, but it was not notably affected by the incorporation of CF. This incorporation (mass fraction 0.02) hardly modified the TGA curve of the TPS films, only slightly delaying the loss of glycerol in the first mass loss step, probably due to the enhanced retention of glycerol brought about by fibre interactions. The mechanism proposed for starch thermo-degradation is a non-oxidative process, which starts first with a scission of glycosidic bonds and the formation of the glycosidic radicals; the starch macromolecules are not directly converted into low molecular weight volatile products, char and levoglucosan, but undergo intermediate physical and chemical changes (Yang et al., 2013). Thus, the depolymerisation of the starch macromolecules takes place with the formation of β-(1,6) anhydro d-glucopyranose (levoglucosan), 2-furaldehyde (furfural) and a range of lower molecular-weight volatile and gaseous fragmentation products (Danilovas et al., 2014). The typical temperature at which the main polymer degradation occurs is in the range of 250–350 °C (Danilovas et al., 2014), as also observed in the film samples. Nevertheless, although all the films with extracts exhibited the main thermo-degradation peak at a temperature about 30 °C lower than that of the extract-free films, this difference was not significantly dependent on the concentration of the extract in the matrix. Both the onset and peak temperatures were affected. The thermo-degradation temperature falls when the molecular weight of the polymer or its degree of crystallisation decreases. In general, the greater the polymer molar mass and cohesion forces of the matrix, the higher the degradation temperature (Danilovas et al., 2014). Therefore, the reduction in the thermal stability of the starch polymers provoked by the extract compounds could be attributed to the starch depolymerising during thermal processing, which is enhanced when there is extract present in the blend, as reported by Menzel et al. (2020), and commented on above. The different ratio of extract in the blend did not significantly affect the thermal stability of the starch films, which suggests that depolymerising occurred to a similar degree in every case. A similar response was also observed for the T_g values of the starch matrix, as a function of the extract concentration, which also points to a similar degree of polymer hydrolysis, regardless of the concentration of extract in the blend. The last degradation step of the starch films, at between 400 and 600 °C, was attributed to the degradation of the first step fragmentation products (Danilovas et al. 2014) and the small differences between samples may be due to the contribution of the most thermostable fractions of the incorporated extract.

The TGA curve of the pure extract revealed the different steps of weight loss prior to and after the main polymer degradation step. The observed peaks in the DTGA curves allow for a better identification of the four mass loss steps: the first (up to about 125 °C) could be attributed to the loss of bounded water (6 % mass loss), the second (125–195 °C) could be assigned to the degradation of low molecular compounds, such as sugars and phenolic compounds (6 % mass loss), the third broad event (46 % mas loss), at between 195 and 400 °C, could be mainly attributed to the degradation of the hemicellulose fractions, which degrade at between 150 and 350 °C, and the fourth step, at between 400 and 600 °C, (25 % mass loss), may be ascribed to the residual lignin fraction that undergoes gradual decomposition in the range of 250–500 °C (Collazo-Bigliardi, 2018). The residual mass, 17.3 %, must be mainly attributed to the silica, present in large quantities in rice straw (17 %, Freitas et al., 2021) in which the extract was enriched. The thermal degradation of the cellulose fraction was previously reported (Freitas et al., 2022a), and exhibited two degradation steps; the main first peak at 286 °C, attributed to the cellulose and residual hemicellulose degradation, and the second at 340–500 °C, attributed to the degradation of the residual lignin and the fragmentation products formed in the first step (Theng et al., 2017).

Therefore, thermal analysis revealed changes in the amorphous phase of the starch films associated with the partial hydrolysis of starch polymers by the action of the RS extract that favoured film plasticisation while reducing the thermal stability of the polymeric matrix.

3.3. Water relations, and mechanical and barrier properties of the films

The incorporation of CF and RS extracts into TPS films affected water relations (water sorption and solubility), tensile behaviour and the barrier capacity of the TPS films, which would, in turn, affect their functionality as packaging materials. Table 2 shows the equilibrium moisture content and water solubility of the films, where the promoted changes can be observed. Other authors (Avérous et al., 2001a; Freitas et al., 2021; Wang et al., 2018) reported that cellulose fibres decreased the moisture diffusion coefficient and sorption capacity of starch composites as the fibre content increased. These effects were attributed to the hydrogen bonds formed between the matrix phase and the fibre phase within the composite, which blocks part of the active sites of the matrix for water interactions and adsorption. However, at the low ratio of fibres incorporated into the films, no significant differences in the equilibrium moisture content were observed for the extract-free films.

Table 2
Moisture, water solubility, oxygen permeability (OP), and water vapour permeability (WVP) of thermoplastic starch films with different contents of CF (0% and 3% wt.) and RS extract (0, 4, 6, and 8 % wt.).

Film	Moisture content (%, d. b.)	Solubility (g soluble film/100 g film)	OP ($x10^{14}$) ($cm^3.m^{-1}.s^{-1}.Pa^{-1}$)	WVP ($mm.g.kPa^{-1}.h^{-1}.m^{-2}$)
TPS	$8.3 \pm 0.2^{a,1}$	$42.4 \pm 1.6^{a,1}$	$8.6 \pm 0.2^{a,1}$	$6.3 \pm 0.2^{b,1}$
TPS-4	$8.2 \pm 0.2^{a,1}$	$45.2 \pm 1.2^{a,1}$	$7.8 \pm 0.1^{b,1}$	$7.9 \pm 0.3^{a,1}$
TPS-6	$8.5 \pm 0.2^{a,1}$	$44.8 \pm 3.7^{a,1}$	$7.4 \pm 0.1^{c,1}$	$7.8 \pm 0.3^{a,1}$
TPS-8	$8.1 \pm 0.1^{a,1}$	$45.2 \pm 0.6^{a,1}$	$7.7 \pm 0.2^{bc,1}$	$7.6 \pm 0.1^{a,1}$
TPScf	$8.3 \pm 0.1^{a,1}$	$38.6 \pm 1.2^{b,2}$	$6.3 \pm 0.1^{a,2}$	$5.9 \pm 0.2^{b,2}$
TPScf-4	$7.7 \pm 0.2^{b,2}$	$47.6 \pm 2.6^{a,1}$	$6.9 \pm 0.1^{a,2}$	$7.2 \pm 0.2^{a,2}$
TPScf-6	$7.7 \pm 0.1^{b,2}$	$45.6 \pm 0.7^{a,1}$	$6.8 \pm 0.5^{a,2}$	$7.1 \pm 0.2^{a,2}$
TPScf-8	$7.8 \pm 0.1^{b,2}$	$42.7 \pm 3.1^{ab,1}$	$6.7 \pm 0.2^{a,2}$	$6.8 \pm 0.1^{a,2}$

Different subscript letters indicate significant differences between samples of the same group (TPS or TPScf films). Different numbers indicate significant differences between TPS and TPScf samples with the same ratio of RS extract (Tukey test, $p < 0.05$).

The incorporation of extracts into fibre-free TPS films did not produce any significant changes in their equilibrium moisture content either. In contrast, the incorporation of extracts into TPS films containing fibre decreased the equilibrium water content, which suggests a notable reduction in the number of active points for water adsorption in the films, probably due to the enhancement of internal hydrogen bonding within the matrix.

The water solubility of the films was only significantly reduced in the films with CF. This reduction has also been reported by other authors (Avérous et al., 2001; Fourati et al., 2020) and can be explained by the insoluble nature of CF and its bonding to the starch matrix through –OH groups, reducing the availability of the starch chains to interact with the water molecules. In contrast, the incorporation of a RS extract tends to slightly enhance the film's solubility, regardless of its concentration. This can be explained by the water solubility of the extract compounds, as well as by the partial hydrolyses of amylose chains, deduced from the thermal analyses, which would promote the starch matrix solubility.

As concerns the barrier capacity of the films, the RS extract enhanced the oxygen barrier capacity but worsened the water vapour barrier of the films, regardless of its concentration. Nevertheless, when films contained CF, the OP values of the films decreased, and these lower values were maintained when the RS extract was incorporated in different ratios. CF also reduced the WVP values that were enhanced when the RS extract was added. Therefore, CF improved the water vapour and oxygen barrier capacities of the films regardless of whether they contain RS extract or not, although slightly higher values of WVP were obtained when the films did contain RS extract. The permeability values of the matrix depended on both permeant solubility and diffusion within the matrix. The incorporation of CF promoted the tortuosity factor for mass transfer purposes and thus reduced the diffusion coefficient. Likewise, the new molecular interactions within the matrix when CF and RS extracts were incorporated could affect the permeant solubility parameter. In the case of films with CF, the permeation of both water and oxygen molecules was inhibited, as reflected in the reduction in the OP and WVP. For films with a RS extract, the permeability of water molecules was enhanced probably due to the plasticisation of the matrix that promoted molecular mobility and diffusion-controlled processes. In contrast, when both RS extract and CF were present in the films, the OP values did not significantly increase with respect to what was obtained for TPScf films; the WVP values, however, were higher, although still lower than the corresponding values of the films without CF. Oun et al. (2022) also found a marked WVP reduction when they incorporated cellulose nanocrystals and aronia (*Aronia melanocarpa*) extract in polyvinyl alcohol/chitosan-based films. The authors reported that the presence of nanocrystals increased the tortuosity factor, while the aronia extract favoured the interchain interactions between polymers, thus also reducing the WVP of the films.

Fig. 2b shows the typical stress–strain curves of the different film formulations with the characteristic tensile parameters (embedded table): elastic modulus (EM) and tensile (TS) and elongation (EB) at break. As observed in previous studies analysing starch-fibre composites (Adeyi et al., 2021; Collazo-Bigliardi et al., 2019), the incorporation of CF into the TPS films led to a significant reinforcement effect, greatly promoting the strength of the films. Although the EM values increased by almost 200 % and the TS by about 100 %, the films became less extensible (EB decreased by almost 60 %) ($p < 0.05$). This reinforcing effect was previously observed in the TPS matrices with the same CF concentration, thus demonstrating the good properties of CF as a reinforcing agent for starch films (Freitas et al., 2021). A slight reinforcement capacity was also observed for the RS extract in TPS films, but to a much lesser extent than that of fibres. However, this effect was not observed for the highest extract concentration. Thus, films with 4 and 6 % of RS extracts exhibited EM values that were 40 % higher ($p < 0.05$) than those of TPS films, whereas the EM value of films with 8 % extract did not significantly differ from that of TPS films. As concerns the resistance to break (TS values), all the extract concentrations increased the TS values by about 20 %, without there being any significant changes in the film's stretchability. In films containing CF, the incorporation of the extract promoted the films extensibility by about 60 %, while reducing the resistance to break (slightly) and the EM (by about 45–60 % depending on the extract concentration).

This behaviour reflects the fact that the extract compounds were able to interact with the starch chains, probably through induced interchain cross-linking, thus hindering the intermolecular motion, enhancing the cohesion forces of the matrix, and promoting film stiffness. In this sense, the RS extract is rich in phenolic acids, mainly ferulic and *p*-cumaric acids (Menzel et al., 2019), that can form interchain hydrogen bonds, enhancing the strength of the starch matrices. A great number of studies reported the cross-linking activity of ferulic acid with different polysaccharides and proteins (Hadrich et al., 2020; Li et al., 2019; Yerramathi et al., 2021). Nevertheless, when the extract solids reach a limit in the film, the cohesion forces could weaken, probably due to the excess of the non-film-forming material that interferes with the chain association.

In contrast, the RS extract seems to inhibit the reinforcing capacity of fibres in the films with CF. This seems to point to the bonding of extract compounds to the cellulosic hydroxyls or to the starch hydroxyls, thus limiting the starch-cellulose bonding ability and, therefore, the fibre reinforcing capacity. Hydrogen bonding between fibres and the polymer represents a key factor in the reinforcement of fibre composites. Avérous et al. (2001) demonstrated the different reinforcing effects of leafwood cellulose fibres on LDPE (no fibre-polymer interactions) and TPS (hydrogen bond formation) films. The ratios of EM and TS of the composites with respect to the fibre-free polymers were notably higher in the case of starch than for LDPE composites. Therefore, it can be assumed that the presence of the RS extract in the films inhibited the fibre-polymer interactions, thus reducing the reinforcing effect. Cellulose fibres at 3 % with respect to starch had a notable reinforcing capacity in the starch matrix, as deduced in a previous study (Freitas et al., 2021). Nevertheless, in the presence of extract, this capacity was undermined, which suggests that fibres also interact with the extract compounds, limiting their capacity to reinforce the polymer matrix.

3.4. Antioxidant capacity of the films and prevention of sunflower oil oxidation.

Table 3 shows the quantity of total phenolic compounds (TPC)

Table 3
Total phenolic content (mg GAE / g film) and DPPH scavenging capacity (EC_{50}) of the films containing different ratios of RS extract (0, 4, 6, and 8% wt.) with and without CF. %GAE recovered with respect to what was initially incorporated into the film and EC_{50} referred per mg of the extract incorporated into the films were also included.

Formulation	TPC (mg GAE/g film)	TPC (%GAE released)	EC_{50} (mg film/mg DPPH)	EC_{50} (mg extract/mg DPPH)
TPS	n.d.	n.d.	n.d.	n.d.
TPS-4	$1.10 \pm 0.02^{c,1}$	$74.4 \pm 1.7^{b,1}$	$85.4 \pm 4.3^{a,1}$	$3.4 \pm 0.2^{c,1}$
TPS-6	$1.63 \pm 0.02^{b,1}$	$73.3 \pm 1.0^{b,1}$	$75.0 \pm 0.2^{b,1}$	$4.5 \pm 0.1^{b,1}$
TPS-8	$2.63 \pm 0.14^{a,1}$	$89.0 \pm 5.0^{a,2}$	$50.5 \pm 1.1^{c,1}$	$4.0 \pm 0.1^{a,1}$
TPScf	n.d.	n.d.	n.d.	n.d.
TPScf-4	$1.22 \pm 0.06^{c,2}$	$83.0 \pm 4.0^{b,2}$	$113.0 \pm 4.0^{a,2}$	$4.5 \pm 0.1^{a,2}$
TPScf-6	$2.14 \pm 0.03^{b,2}$	$96.2 \pm 1.2^{a,2}$	$69.0 \pm 4.0^{b,2}$	$4.1 \pm 0.2^{a,1}$
TPScf-8	$2.40 \pm 0.04^{a,2}$	$80.8 \pm 1.5^{b,1}$	$40.3 \pm 1.1^{c,2}$	$3.2 \pm 0.1^{b,2}$

Different subscript letters indicate significant differences between samples of the same group (TPS or TPScf films). Different numbers indicate significant differences between TPS and TPScf samples with the same ratio of RS extract (Tukey test, $p < 0.05$).

released from the different films in the aqueous medium, and their corresponding DPPH radical scavenging capacity. The results reflected the TPC released per mass unit of film and the corresponding percentage with respect to what was initially incorporated into the film, considering both the extract content and its TPC value. In no case was the total delivery of the incorporated phenolics achieved; however, higher percentages were obtained from the films with 8 % extract without CF and from every film with CF. The incomplete delivery could be attributed to the partial degradation of these compounds during the thermal processing of the films.

As expected, the radical scavenging capacity of the films, expressed as the ratio of film to DPPH necessary to inhibit the radical activity by 50 % (EC_{50}) increased as the extract ratio rose in the film, since lower amounts of EC_{50} were obtained. When this parameter was referred to the respective mass of extract in the different films, no absolutely constant values were obtained, these being lower than what was determined in the pure extract (6.3 ± 0.3). This indicates that the radical scavenging capacity of the extract after the film processing was enhanced (lower EC_{50} values than the initial extract: 3.95 as mean value) probably due to the formation of more active compounds either during the film thermoprocessing (at 130 and 160 °C, respectively, for melt blending and compression moulding) in which new antioxidant compounds could be released from the lignin fraction of the extract (Wanyo et al., 2014) or in the thermo-formation of new antioxidant compounds through Maillard or caramelisation reactions during the melt blending step, as reported by other authors (Plaza et al., 2010) for different plant extracts when submitted to high temperature processes. Therefore, although no total recovery of phenolics was achieved from the thermoprocessed films, their radical scavenging capacity was enhanced, and so was their antioxidant activity.

To validate the antioxidant capacity in real foods, the ability of the films containing extracts to prevent sunflower oil oxidation was analysed in an accelerated oxidation test (Talón et al., 2019). To this end, film bags of TPS with 8 % extract with and without CF (TPS-8 and TPScf-8 formulations) were selected to obtain mono-dose oil samples based on their higher antioxidant capacity and lower oxygen permeability. For comparison purposes, mono-dose bags of the corresponding films without extract were also prepared and analysed as to their peroxide index and TBARS value as a function of the storage time under oxidation conditions with UV light. Fig. 3 shows the development of the controlled oxidation parameters for these four oil samples and the control sample in an open plate. The peroxide index (Fig. 3a) increased very quickly in the open samples, demonstrating the oxidative conditions of the test, whereas in packaged oil the peroxide formation was much slower since the bag material limited the oxygen transfer, since all the films exhibited relatively low values of OP. Likewise, the bags with RS extracts delayed the peroxide formation even more, which must be attributable to the antioxidant effect of the extract compounds. Consequently, the TBARS index values (Fig. 3b), from the secondary oxidation phase, were lower in packaged oil samples and notably reduced when the bags contained RS extracts. When the RS extract was present in the films, it was not possible to observe significant differences between the films with CF and those without, but TPS bags with CF were more efficient at limiting oil oxidation than TPS without CF. This can be attributed to the reduction in OP brought about by CF incorporation, as well as the lower light transmittance of the TPScf films, which protect oil from light induced oxidation. In the case of films with RS extract, the high capacity of the extract to limit oil oxidation masked the possible differences associated with the lower OP of TPScf-8 films, compared to TPS-8. Likewise, both films with extracts exhibited a high degree of UV light absorption, which will also contribute to the antioxidant capacity of the material. Therefore, the incorporation of both CF and active extract from the RS agri-food residue into starch mono-dose bags constituted efficient protection for the purposes of delaying the oxidation of sunflower oil throughout storage.

4. Conclusions

New functionalities of thermoplastic TPS films were achieved when RS fractions were incorporated. CF promoted the film strength and is an effective reinforcing agent at 3 % with respect to thermoplastic starch. The incorporation of RS aqueous extract into both TPS and reinforced TPS films, produced more plasticised, less thermostable matrices, but provided them with strong antioxidant and UV absorption capacity, which permits the prevention of sunflower oil oxidation. CF enhanced the oxygen and water vapour barrier capacity of the films with and without RS extracts, while reinforcing their mechanical resistance and elastic modulus. Therefore, obtaining fractions from RS that are useful for the purposes of improving food packaging materials, such as starch films, represents a good strategy for the valorisation of this waste, while at the same time opening up new windows in the development of active biodegradable materials for food packaging and preservation.

CRediT authorship contribution statement

Pedro A.V. Freitas: Conceptualization, Methodology, Formal analysis, Investigation, Writing – original draft, Writing – review & editing. **Consuelo González-Martínez:** Conceptualization, Methodology, Formal analysis, Investigation, Writing – original draft, Writing – review & editing. **Amparo Chiralt:** Conceptualization, Methodology, Formal analysis, Investigation, Writing – original draft, Writing – review & editing.

Declaration of Competing Interest

The authors declare that they have no known competing financial interests or personal relationships that could have appeared to influence the work reported in this paper.

Data availability

The authors do not have permission to share data.

Acknowledgment

This work is supported by Generalitat Valenciana [grant number GrisoliaP/2019/115] and project PID2019-105207RB-I00/AEI/10.13039/501100011033.

References

ASTM. (2010). D3985-05 oxygen gas transmission rate through plastic film and sheeting using a coulometric sensor. *Annual Book of ASTM Standards, C, 1–7*. https://doi.org/10.1520/D3985-05.2

ASTM. (2012). Standard test method for tensile properties of thin plastic sheeting. ASTM D882–12. *American Society for Testing and Materials, 12*.

Adeyi, A. J., Durowoju, M. O., Adeyi, O., Oke, E. O., Olalere, O. A., & Ogunsola, A. D. (2021). Momordica augustisepala L. stem fibre reinforced thermoplastic starch: Mechanical property characterization and fuzzy logic artificial intelligent modelling. *Results Engineering, 10*, Article 100222. https://doi.org/10.1016/j.rineng.2021.100222

Avérous, L., Fringant, C., & Moro, L. (2001). Plasticized starch–cellulose interactions in polysaccharide composites. *Polymer, 42*(15), 6565–6572. https://doi.org/10.1016/S0032-3861(01)00125-2

Balakrishnan, P., Gopi, S., Geethamma, V. G., Kalarikkal, N., & Thomas, S. (2018). Cellulose nanofiber vs nanocrystals from pineapple leaf fiber: a comparative studies on reinforcing efficiency on starch nanocomposites. *Macromolecular Symposia, 380*(1), 1800102. https://doi.org/10.1002/masy.201800102

Brand-Williams, W., Cuvelier, M. E., & Berset, C. (1995). Use of a free radical method to evaluate antioxidant activity. *LWT - Food Science and Technology, 28*(1), 25–30. https://doi.org/10.1016/S0023-6438(95)80008-5

Carvalho, A. J. F., Zambon, M. D., Curvelo, A. A. S., & Gandini, A. (2003). Size exclusion chromatography characterization of thermoplastic starch composites 1. Influence of plasticizer and fibre content. *Polymer Degradation and Stability, 79*(1), 133–138. https://doi.org/10.1016/S0141-3910(02)00265-3

Chen, X., Yu, J., Zhang, Z., & Lu, C. (2011). Study on structure and thermal stability properties of cellulose fibers from rice straw. *Carbohydrate Polymers, 85*(1), 245–250. https://doi.org/10.1016/j.carbpol.2011.02.022

Collazo-Bigliardi, S. (2018). Isolation and characterisation of microcrystalline cellulose and cellulose nanocrystals from coffee husk and comparative study with rice husk. *Carbohydrate Polymers, 11*.

Collazo-Bigliardi, S., Ortega-Toro, R., & Chiralt, A. (2019). Improving properties of thermoplastic starch films by incorporating active extracts and cellulose fibres isolated from rice or coffee husk. *Food Packaging and Shelf Life, 22*, Article 100383. https://doi.org/10.1016/j.fpsl.2019.100383

Dalnoki-Veress, K., Forrest, J. A., Murray, C., Gigault, C., & Dutcher, J. R. (2001). Molecular weight dependence of reductions in the glass transition temperature of thin, freely standing polymer films. *Physical Review E, 63*(3), Article 031801. https://doi.org/10.1103/PhysRevE.63.031801

Danilovas, P. P., Rutkaite, R., & Zemaitaitis, A. (2014). Thermal degradation and stability of cationic starches and their complexes with iodine. *Carbohydrate Polymers, 112*, 721–728. https://doi.org/10.1016/j.carbpol.2014.06.038

Fourati, Y., Magnin, A., Putaux, J.-L., & Boufi, S. (2020). One-step processing of plasticized starch/cellulose nanofibrils nanocomposites via twin-screw extrusion of starch and cellulose fibers. *Carbohydrate Polymers, 229*, Article 115554. https://doi.org/10.1016/j.carbpol.2019.115554

Freitas, P. A. V., Arias, C. I. L. F., Torres-Giner, S., González-Martínez, C., & Chiralt, A. (2021). Valorization of rice straw into cellulose microfibers for the reinforcement of thermoplastic corn starch films. *Applied Sciences, 11*(18), 8433. https://doi.org/10.3390/app11188433

Freitas, P. A. V., González-Martínez, C., & Chiralt, A. (2020). Application of ultrasound pre-treatment for enhancing extraction of bioactive compounds from rice straw. *Foods, 9*(11), 1657. https://doi.org/10.3390/foods9111657

Freitas, P. A. V., González-Martínez, C., & Chiralt, A. (2022a). Applying ultrasound-assisted processing to obtain cellulose fibres from rice straw to be used as reinforcing agents. *Innovative Food Science & Emerging Technologies, 76*, Article 102932. https://doi.org/10.1016/j.ifset.2022.102932

Freitas, P. A. V., Gil, N. J. B., González-Martínez, C., & Chiralt, A. (2022b). Antioxidant poly (lactic acid) films with rice straw extract for food packaging applications. *Food Packaging and Shelf Life*. In press.

Hadrich, A., Dulong, V., Rihouey, C., Labat, B., Picton, L., & Le Cerf, D. (2020). Biomimetic hydrogel by enzymatic crosslinking of pullulan grafted with ferulic acid. *Carbohydrate Polymers, 250*, Article 116967. https://doi.org/10.1016/j.carbpol.2020.116967

Li, K., Zhu, J., Guan, G., & Wu, H. (2019). Preparation of chitosan-sodium alginate films through layer-by-layer assembly and ferulic acid crosslinking: Film properties, characterization, and formation mechanism. *International Journal of Biological Macromolecules, 122*, 485–492. https://doi.org/10.1016/j.ijbiomac.2018.10.188

Mak, T. M. W., Xiong, X., Tsang, D. C. W., Yu, I. K. M., & Poon, C. S. (2020). Sustainable food waste management towards circular bioeconomy: Policy review, limitations and opportunities. *Bioresource Technology, 297*, Article 122497. https://doi.org/10.1016/j.biortech.2019.122497

Menzel, C. (2020). Improvement of starch films for food packaging through a three-principle approach: Antioxidants, cross-linking and reinforcement. *Carbohydrate Polymers, 250*, Article 116828. https://doi.org/10.1016/j.carbpol.2020.116828

Menzel, C., González-Martínez, C., Chiralt, A., & Vilaplana, F. (2019). Antioxidant starch films containing sunflower hull extracts. *Carbohydrate Polymers, 214*, 142–151. https://doi.org/10.1016/j.carbpol.2019.03.022

Menzel, C., González-Martínez, C., Vilaplana, F., Diretto, G., & Chiralt, A. (2020). Incorporation of natural antioxidants from rice straw into renewable starch films. *International Journal of Biological Macromolecules, 146*, 976–986. https://doi.org/10.1016/j.ijbiomac.2019.09.222

Mochane, M. J., Magagula, S. I., Sefadi, J. S., & Mokhena, T. C. (2021). A review on green composites based on natural fiber-reinforced polybutylene succinate (PBS). *Polymers, 13*(8), 1200. https://doi.org/10.3390/polym13081200

Ng, H.-M., Sin, L. T., Tee, T.-T., Bee, S.-T., Hui, D., Low, C.-Y., & Rahmat, A. R. (2015). Extraction of cellulose nanocrystals from plant sources for application as reinforcing agent in polymers. *Composites Part B: Engineering, 75*, 176–200. https://doi.org/10.1016/j.compositesb.2015.01.008

Ordoñez, R., Atarés, L., & Chiralt, A. (2021). Physicochemical and antimicrobial properties of cassava starch films with ferulic or cinnamic acid. *LWT, 144*, Article 111242. https://doi.org/10.1016/j.lwt.2021.111242

Oun, A. A., Shin, G. H., & Kim, J. T. (2022). Antimicrobial, antioxidant, and pH-sensitive polyvinyl alcohol/chitosan-based composite films with aronia extract, cellulose nanocrystals, and grapefruit seed extract. *International Journal of Biological Macromolecules, 213*, 381–393. https://doi.org/10.1016/j.ijbiomac.2022.05.180

Papastergiadis, A., Mubiru, E., Van Langenhove, H., & De Meulenaer, B. (2012). Malondialdehyde measurement in oxidized foods: evaluation of the spectrophotometric thiobarbituric acid reactive substances (TBARS) test in various foods. *Journal of Agricultural and Food Chemistry, 60*(38), 9589–9594. https://doi.org/10.1021/jf302451c

Perumal, A. B., Sellamuthu, P. S., Nambiar, R. B., & Sadiku, E. R. (2018). Development of polyvinyl alcohol/chitosan bio-nanocomposite films reinforced with cellulose nanocrystals isolated from rice straw. *Applied Surface Science, 449*, 591–602. https://doi.org/10.1016/j.apsusc.2018.01.022

Plaza, M., Amigo-Benavent, M., del Castillo, M. D., Ibáñez, E., & Herrero, M. (2010). Facts about the formation of new antioxidants in natural samples after subcritical water extraction. *Food Research International, 43*(10), 2341–2348. https://doi.org/10.1016/j.foodres.2010.07.036

Sá, N. M. S. M., Mattos, A. L. A., Silva, L. M. A., Brito, E. S., Rosa, M. F., & Azeredo, H. M. C. (2020). From cashew byproducts to biodegradable active materials: Bacterial cellulose-lignin-cellulose nanocrystal nanocomposite films. *International Journal of Biological Macromolecules, 161*, 1337–1345. https://doi.org/10.1016/j.ijbiomac.2020.07.269

Sluiter, A. (2008). Determination of Structural Carbohydrates and Lignin in Biomass: Laboratory Analytical Procedure (LAP); Issue Date: April 2008; Revision Date: July 2011 (Version 07-08-2011). *Technical Report*, 18.

Talón, E., Trifkovic, K. T., Nedovic, V. A., Bugarski, B. M., Vargas, M., Chiralt, A., & González-Martínez, C. (2017). Antioxidant edible films based on chitosan and starch containing polyphenols from thyme extracts. *Carbohydrate Polymers, 157*, 1153–1161. https://doi.org/10.1016/j.carbpol.2016.10.080

Talón, E., Vargas, M., Chiralt, A., & González-Martínez, C. (2019). Antioxidant starch-based films with encapsulated eugenol. *Application to sunflower oil preservation. LWT, 113*, Article 108290. https://doi.org/10.1016/j.lwt.2019.108290

Tavares, K. M., de Campos, A., Mitsuyuki, M. C., Luchesi, B. R., & Marconcini, J. M. (2019). Corn and cassava starch with carboxymethyl cellulose films and its mechanical and hydrophobic properties. *Carbohydrate Polymers, 223*, Article 115055. https://doi.org/10.1016/j.carbpol.2019.115055

Theng, D., Arbat, G., Delgado-Aguilar, M., Ngo, B., Labonne, L., Evon, P., & Mutjé, P. (2017). Comparison between two different pretreatment technologies of rice straw fibers prior to fiberboard manufacturing: Twin-screw extrusion and digestion plus defibration. *Industrial Crops and Products, 107*, 184–197. https://doi.org/10.1016/j.indcrop.2017.05.049

Wang, Z., Qiao, X., & Sun, K. (2018). Rice straw cellulose nanofibrils reinforced poly (vinyl alcohol) composite films. *Carbohydrate Polymers, 197*, 442–450. https://doi.org/10.1016/j.carbpol.2018.06.025

Wanyo, P., Meeso, N., & Siriamornpun, S. (2014). Effects of different treatments on the antioxidant properties and phenolic compounds of rice bran and rice husk. *Food Chemistry, 157*, 457–463. https://doi.org/10.1016/j.foodchem.2014.02.061

Yang, Z., Liu, X., Yang, Z., Zhuang, G., Bai, Z., Zhang, H., & Guo, Y. (2013). Preparation and formation mechanism of levoglucosan from starch using a tubular furnace pyrolysis reactor. *Journal of Analytical and Applied Pyrolysis, 102*, 83–88. https://doi.org/10.1016/j.jaap.2013.03.012

Yerramathi, B. B., Kola, M., Annem Muniraj, B., Aluru, R., Thirumanyam, M., & Zyryanov, G. V. (2021). Structural studies and bioactivity of sodium alginate edible films fabricated through ferulic acid crosslinking mechanism. *Journal of Food Engineering, 301*, Article 110566. https://doi.org/10.1016/j.jfoodeng.2021.110566